Environmental Science and Ecotechnology 19 (2024) 100324

Contents lists available at ScienceDirect

Environmental Science and Ecotechnology

journal homepage: www.journals.elsevier.com/environmental-science-and-ecotechnology/

Original Research

H_2 mediated mixed culture microbial electrosynthesis for high titer acetate production from CO_2

Yanhong Bian [a, b], Aaron Leininger [a, b], Harold D. May [b], Zhiyong Jason Ren [a, b, *]

[a] Department of Civil and Environmental Engineering, Princeton University, 86 Olden St, Princeton, NJ, 08544, United States
[b] Andlinger Center for Energy and the Environment, Princeton University, 86 Olden St., Princeton, NJ, 08544, United States

ARTICLE INFO

Article history:
Received 7 May 2023
Received in revised form
26 September 2023
Accepted 27 September 2023

Keywords:
Microbial electrosynthesis
Indirect electron transfer
CO_2 electrolysis
VFAs production

ABSTRACT

Microbial electrosynthesis (MES) converts CO_2 into value-added products such as volatile fatty acids (VFAs) with minimal energy use, but low production titer has limited scale-up and commercialization. Mediated electron transfer via H_2 on the MES cathode has shown a higher conversion rate than the direct biofilm-based approach, as it is tunable via cathode potential control and accelerates electrosynthesis from CO_2. Here we report high acetate titers can be achieved via improved *in situ* H_2 supply by nickel foam decorated carbon felt cathode in mixed community MES systems. Acetate concentration of 12.5 g L^{-1} was observed in 14 days with nickel-carbon cathode at a poised potential of −0.89 V (vs. standard hydrogen electrode, SHE), which was much higher than cathodes using stainless steel (5.2 g L^{-1}) or carbon felt alone (1.7 g L^{-1}) with the same projected surface area. A higher acetate concentration of 16.0 g L^{-1} in the cathode was achieved over long-term operation for 32 days, but crossover was observed in batch operation, as additional acetate (5.8 g L^{-1}) was also found in the abiotic anode chamber. We observed the low Faradaic efficiencies in acetate production, attributed to partial H_2 utilization for electrosynthesis. The selective acetate production with high titer demonstrated in this study shows the H_2-mediated electron transfer with common cathode materials carries good promise in MES development.

1. Introduction

Many countries and industries are pledging net-zero emissions to combat climate change and its devastating impacts [1]. Carbon capture and utilization are critical to this mission and help achieve a circular carbon economy by converting CO_2 into value-added products [2,3]. CO_2, as an alternative carbon source, can be converted to various fuels, chemicals, and materials via photo-, electro-, thermal-, and biological conversion pathways. Among these processes, microbial electrochemical CO_2 reduction using microbes has a good potential, characterized by its high selectivity, low energy use, self-sustaining nature, and co-benefits with waste treatment [4].

Microbial electrosynthesis (MES) uses electroactive bacteria and homoacetogens to mediate CO_2 reduction to volatile fatty acids (VFAs), particularly acetate, with low electricity input from the cathode [5]. It has been reported that the primary route of electron transfer for MES from CO_2 is indirect electron transfer, which operates via mediators such as *in situ* generated H_2, CO, formate, or other small molecules [6–8]. Although there is a potential for certain species to directly uptake electrons from the cathode for CO_2 reduction to acetate, empirical evidence substantiating this mechanism is presently sparse [5,9,10]. The mechanisms of direct electron transfer for MES from CO_2 remain to be elucidated. However, it is increasingly recognized that indirect electron transfer via mediators holds significant potential as it delivers a high CO_2 conversion rate and current density [11,12]. In addition, these mediated processes allow reactions to occur in the bulk solution, overcoming the limitation posed by the biofilm and cathode surface area and facilitating reaction rate and process application. The importance of H_2 route in MES has been identified by comparing the microbial CO_2 reduction under two different cathode potentials without (−0.36 V vs. standard hydrogen electrode, SHE) and with H_2 evolution (−0.66 V vs. SHE). Notably, the H_2-mediated process demonstrated more than ten times higher current density and a significant increase in acetate production from 0 to 244 mg L^{-1} [6].

* Corresponding author. Department of Civil and Environmental Engineering, Princeton University, 86 Olden St, Princeton, NJ, 08544, United States.
E-mail address: zjren@princeton.edu (Z.J. Ren).

https://doi.org/10.1016/j.ese.2023.100324

As the primary liquid product of MES, the acetate titers reported in previous studies range from less than 0.5 to 17.5 g L^{-1}, most of which are lower than 10 g L^{-1} [4,13]. High acetate titer values of 13.5 and 17.5 g L^{-1} have been obtained in a three-chamber MES with *in situ* extraction operated for 43 days and a flow-through MES with a high CO_2 loading rate operated for 164 days, respectively [14,15].

Recognizing that H_2-mediated VFAs production in MES can boost productivity and overcome the electrochemical surface barrier, developing efficient H_2 production and conversion processes is critical for scaling and applying the MES technology in the real world. Studies have tested a variety of cathode and catalyst materials to improve H_2 production, including carbon felt coated with Pt NPs/rGO, TiO_2, MoC and Rh, Fe_xMnO_y, Si wafer coated with CoP, MoS_2, and NiMo, and nickel hollow fiber coated with nanotube [11,16–19]. In many cases, the increased H_2 production didn't necessarily correspond with higher VFAs concentrations and might result in low Faradaic efficiency due to insufficient H_2 utilization. This could arise from a divergence between the H_2 generate rate, determined by the applied potential and the cathode material, and the rate at which H_2 is utilized, which is contingent upon microbial H_2 uptake coupled with CO_2 reduction [7]. Therefore, it's important to investigate the impacts of materials and operation conditions, such as cathode potential, to minimize the discrepancy between H_2 generation and utilization and improve CO_2 conversion.

Nickel foam has garnered considerable attention as a cathode material in electrochemical systems for H_2 production. This increased focus stems from its porous three-dimensional structure, good catalytic ability, and low cost. To enhance CO_2 reduction rates and biochemical production in MES, nickel foam coated with graphene or multiwalled carbon nanotubes has been utilized as an MES cathode, improving surface area and biocompatibility [20,21]. However, surface-modified materials have some drawbacks, including a relatively complex preparation process and low mechanical strength, which limits their application on a large scale. Thus, developing engineeringly relevant materials and processes would be desired for applications. Carbon-based materials, such as carbon felt, are commonly chosen as electrodes for microbial electrochemical systems due to their porous configuration, good biocompatibility, and corrosion resistance. A combination of commercial carbon felt and nickel foam may be an alternative for MES cathode, which could simultaneously enhance *in situ* H_2 production and microbial electrosynthesis. In addition, the long-term operation of cathode materials on MES performance needs to be investigated to obtain a higher titer.

In this study, we investigated VFAs production from CO_2 in MES with a mixed microbial culture by employing a hybrid cathode composed of scalable carbon felt coupled with common metal materials, such as nickel foam and stainless steel. We hypothesize such materials hold the best realistic potential in MES for CO_2 reduction, as these low-cost materials can produce tunable H_2 that facilitates autotrophic hematogenesis without causing significant pH changes due to protons consumption. We analyzed and compared the VFAs production from CO_2 by using different combinations of materials under different cathode potentials. A long-term MES operation was also carried out, which proved that high titer acetate can be produced without microbial re-consumption. We also reported an acetate crossover phenomenon during the processes. Microbial community changes were also characterized to reveal the evolution of the microbiomes in long-term operating MES.

2. Materials and methods

2.1. Mixed culture and cultivation conditions

MES reactors were inoculated with enriched mixed cultures. The inoculum mixtures were prepared by adding anaerobic sludge taken from a wastewater treatment plant into a growth medium in a 1:10 ratio in triplicate serum bottles. The serum bottles were incubated at 28 °C with H_2:CO_2 (80:20) in the headspace at 0.5 bar overpressure. The growth medium contained the following: $NaHCO_3$, 4.2 g L^{-1}; NaH_2PO_4, 2.45 g L^{-1}; Na_2HPO_4, 4.575 g L^{-1}; KCl: 0.13 g L^{-1}; NH_4Cl, 0.31 g L^{-1}; yeast extract, 0.5 g L^{-1}; 10 mL vitamin solution; and 10 mL trace element solution [22]. After stable VFAs production was obtained in the serum bottle, the enriched community was used as the inoculum for MES cathode inoculum (Fig. S2). 2-Bromoethanesulfonate (BES, 1 g L^{-1}) was added to the solution to inhibit methanogenesis unless otherwise stated.

2.2. MES reactor configuration and operation

Two-chamber cubic MES reactors were used for microbial CO_2 electrosynthesis as depicted in Supplementary Materials (Fig. S1). The anode and cathode chambers (8 cm × 8 cm × 1.9 cm each) were separated by a cation-exchange membrane (CMI-70000, Membrane International, USA). A mixed metal oxide (MMO, IrO_2/RuO_2) coated titanium mesh (3 cm × 2 cm) was used as the anode electrode due to its low overpotential and good stability for oxygen evolution reaction (OER) [23–25]. Carbon felt (7.5 cm × 7.5 cm × 2 mm) was used as the base cathode electrode. Either a piece of nickel foam (MTI Corporation, USA, thickness: 1.6 mm; surface density: 346 g m^{-2}; porosity: ≥95%) or stainless-steel mesh (316 L, 60 × 60 mesh with wire diameter 0.19 mm) with the same projected area was mechanically attached to the surface of carbon felt by using a titanium wire. The cathode electrode made of carbon felt alone, carbon felt coupled with nickel foam, and carbon felt coupled with stainless steel are named CF, CF-NF, and CF-SSL, respectively. The MES cathode was inoculated using a pre-enriched mixed culture from a serum bottle. The inoculum was obtained by centrifuging 10 mL solution with enriched culture at 8000 g for 10 min, then re-suspending and transferring the concentrated biomass to the MES cathode chamber. The MES reactors were inoculated with pre-enriched inoculum to make an initial optical density at 600 nm (OD_{600}) of ~0.3. Yeast extract was omitted in the catholyte during the MES operation. The anolyte applied in this study was 50 mM Na_2SO_4 with a pH of about 2.2, adjusted by H_2SO_4. Both anolyte and catholyte have a volume of 125 mL and were recirculated using a peristaltic pump with a flow rate of 10 mL min^{-1}. The MES reactors were operated at room temperature (~22 °C) with a constant cathode potential controlled by a potentiostat (VMP3, BioLogic) in a three-electrode configuration. The cathode was used as the working electrode, the anode was the counter electrode, and a Ag/AgCl (3 M KCl) placed in the cathode chamber was used as the reference electrode. To investigate the effects of cathode potential, MES performance under different cathode potentials was tested from −1.1 V to −0.7 V vs. Ag/AgCl with 3 M KCl (−0.89 V to −0.49 V vs. SHE). The long-term tests of MES reactors were operated with cathode potential controlled at −0.89 V vs. SHE. Unless specified differently, all the electrode potentials referenced in this manuscript are in relation to the standard hydrogen electrode (SHE). The current density was normalized to the projected cathode surface area and reported as absolute values. During the batch operation, CO_2 gas was delivered to the catholyte with a constant flow rate of 15 mL min^{-1} to provide a carbon source for microbes in the cathode chamber. All the results were reported based on calculations from two replicate tests.

2.3. Chemical and microscopic characterizations

Liquid samples (1 mL) were withdrawn from the cathode chamber at 1–4 days intervals, and volatile fatty acids were analyzed via a high-performance liquid chromatography (HPLC, Agilent 1260 Infinity II) with Hi-Plex H column and mobile phase of 4 mM H_2SO_4 [26]. The pH of liquid samples was checked with a pH meter (Thermal Scientific). The optical density of the planktonic cells was measured at 600 nm (OD_{600}) using a Genesys Ultraviolet–visible (UV/Vis) spectrophotometer. The Faradaic efficiency (FE) was calculated from the partial current densities of total products detected in the system divided by the total applied current. Gas samples extracted from the headspace of the cathode bottle were collected using a gas bag and analyzed by a gas chromatograph (GC) with a thermal conductivity detector (TCD) when noted. The gas production rate is calculated by measuring gas volume collected over a specific duration.

MES cathode materials with attached microbes after long-term operation were characterized using scanning electron microscopy (Verios 460 XHR SEM). The electrodes from the cathode chamber were fixed for 3 h in 2% glutaraldehyde in a 0.1 M sodium phosphate buffer. Then, the cathodes were washed with 0.1 M phosphate buffer for 1 h, followed by stepwise dehydration in ethanol (25%, 50%, 75%, 90%, 100%) [7,27]. The electrodes were sputter coated with 3 nm of iridium (Leica EM ACE600) before being characterized using SEM.

2.4. Microbial community analysis

Microbial samples from the suspension (planktonic cells) and the cathode electrodes were collected during each period of operation for microbial community analyses. Genomic DNA was extracted from the samples using DNeasy PowerSoil Pro kit (QIAGEN). The preparation of the library and the paired-end amplicon sequencing of the V4 region of the 16S rRNA gene were carried out according to previously described methods [28]. Sequencing analyses were conducted in R using the DADA2 pipeline to obtain amplicon sequence variants (ASVs) [29]. SILVA database (release 138) was used to assign taxonomy, and data were imported into phyloseq R package for microbiome data analysis [30,31].

3. Results and discussions

3.1. MES current density and abiotic H_2 supply

Cyclic voltammetry (CV) tests (1 mV s^{-1}) were performed to determine the electrochemical characteristics of the different cathode electrodes (Fig. 1a). Among the combinations tested, the nickel foam coupled electrode showed the highest reductive current density, which was followed by stainless steel. The carbon felt alone showed the lowest current at all potentials due to the low catalytic ability of carbon materials alone. Based on the CV profile, cathode potentials of −0.89, −0.69, and −0.49 V vs. SHE were selected for MES operation and comparison. MES reactors equipped with these three cathodes (CF, CF-SSL, and CF-NF) were operated under different cathode potentials at each cycle time of 14 days. The averaged current densities were calculated based on the current density between replicates under different cathode potentials (Fig. 1b). The current profile (data not shown here) changed slightly without obvious up-and-down trends during operation. The current densities obtained from the reactors correlated with the CV results under the corresponding cathodes. For example, the highest current density (20.42 ± 1.32 A m^{-2}) was achieved in the group of CF-NF cathode under −0.89 V vs. SHE, and this number is orders of magnitudes higher than reactors using carbon felt cathode ($5.3 \times 10^{-3} \pm 0.5 \times 10^{-3}$ A m^{-2}), which showed poor catalytic ability for H_2 evolution. Abiotic control tests without microbial growth were also conducted at different cathode potentials to test abiotic H_2 production. It was found that an average volumetric H_2 production rate of 1.44×10^{-4} mol L^{-1} min^{-1} was observed with CF-NF cathode at −0.89 V. This rate was approximately 2.95 times the production rate observed from CF-SSL (4.88×10^{-5} mol L^{-1} min^{-1}) and 23 times of that from CF cathode (6.08×10^{-6} mol L^{-1} min^{-1}) at same cathode potential (Table S1). It is noted that the H_2 production rate is not comparable to typical water electrolysis technologies with very high current densities (2000–20000 A m^{-2}), which is attributed to the different nature of electrodes, electrolytes, and cell design [32]. Since H_2 is the targeted electron mediator for microbial CO_2 electrosynthesis, these results provided a good understanding of H_2 supply capability by different cathodes in different operation conditions.

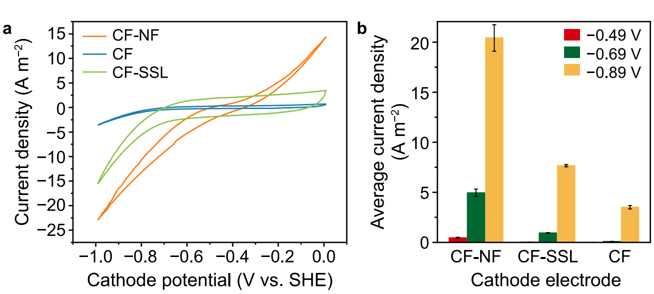

Fig. 1. a, Cyclic voltammetry profiles of different cathode materials without microbes' growth CF-NF: carbon felt composed with nickel foam; CF: carbon felt; CF-SSL: carbon felt composed with stainless steel mesh. **b**, Average current density profiles of MES with different electrodes under different cathode potentials. The error bars represent each group's standard deviation from two replicate tests.

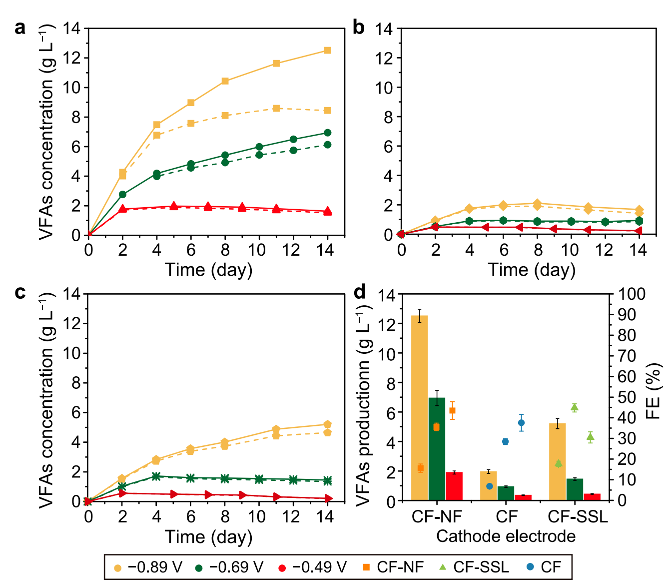

Fig. 2. a–**c**, VFA production in MES using different cathode electrodes and applied cathode potentials: **a**, carbon felt assembled with nickel foam (CF–NF); **b**, carbon felt (CF); **c**, carbon felt assembled with stainless steel mesh (CF-SSL). The solid lines refer to total VFA production, dash lines refer to VFAs detected in the cathode chamber. **d**, VFA production and Faradaic efficiency (FE) of MES under different conditions.

3.2. VFAs production in MES reactors

For all MES reactors equipped with different cathodes, it was observed that the production of VFAs increased as the cathode potential decreased (Fig. 2). The highest VFAs production was observed under the cathode potential of −0.89 V vs. SHE, which was attributed to higher H_2 evolution and current densities [6,33,34]. The highest VFA titer of 12.5 g L^{-1} was obtained in MES with CF-NF electrode after 14-days operation with a maximum acetate production rate of 2.0 g L^{-1} d^{-1}, while lower VFA productions were observed under the same cathode for potential CF-SSL (5.2 g L^{-1} titer with maximum rate of 0.8 g L^{-1} d^{-1}) and CF (1.7 g L^{-1} titer with maximum rate of 0.5 g L^{-1} d^{-1}). This certainly credits to the high catalytic activity of nickel foam for H_2 production, which boosted the supply of electron donors for microbes to metabolize CO_2 reduction [35]. Acetate was the most dominant VFA species among all liquid products, and small amounts of butyrate, propionate, isobutyrate, and isovalerate were also produced (Fig. S3).

Along with the high VFA production in the cathode chamber, we also detected VFAs in the abiotic anode chambers. Acetate was the only detectable VFA species in the anode chambers, and the discrepancy between the solid lines and dash lines shown in Fig. 2a–c depicts the acetate concentration detected in the anode. For example, approximately 3 g L^{-1} of acetate was detected in the anolyte in MES with CF-NF cathode, lowering the residue cathode VFA concentration from 12.5 to 8.5 g L^{-1} (Fig. 2a). The presence of acetate in the anode chamber may result from its migration across the membrane from the cathode. Given that the abiotic anode cannot generate acetate, this ion migration seems a possible explanation. Acetate crossover was also reported in MESs equipped with cation exchange membranes or proton exchange membranes [12,36], as it was found acetate in anion form can also transport across a cation exchange membrane when the concentration gradient between the two chambers is very high. In addition, in some cases, VFA concentration decreased at the end of the cycle, possibly due to the re-consumption of small VFA molecules by some of the microbes in the mixed culture. Measures need to be taken to minimize the migration loss from the catholyte. For example, *in situ*, VFA extraction using membrane contactors or pervaporation or adding an extraction chamber between anode and cathode might be effective approaches to facilitate VFA production and reduce back diffusion by pulling the products out of the cathode chamber, or more selective separators could be used between the anode and cathode chambers [14,37].

Fig. 2d shows the FE of VFAs production in the cathode (total VFAs based on the solid line in Fig. 2a–c). The FE for all groups ranged between 16% and 50%, consistent with the results from most previous studies [16]. Most groups delivered a decreased FE as the cathode potential became more negative, likely due to an oversupply of H_2 surpassing microbial uptake capabilities. However, the MES with CF-SSL electrode showed a slight increase in FE at −0.69 V, suggesting an optimal condition for H_2 utilization at this potential. This enhanced VFA production and reduced H_2 loss, thereby maintaining a relatively higher FE. Higher VFA titers did not necessarily result in higher FE, as VFA conversion depended on many factors, such as CO_2 availability, H_2 availability, and microbial activities. If other factors become limiting factors, the current/H_2 may be oversupplied, leading to lower FEs. VFA production in the cathode has been linked to CO_2 conversion, which can be attributed to either suspended planktonic cells in the catholyte or microbes adhering to the cathode electrode. The OD_{600} of catholyte serves as an indicator for the concentration of microorganisms in the solution. As shown in Fig. S4, the OD_{600} values steadily increased during the operation across most experimental groups, demonstrating a generally positive correlation with VFA production. However, SEM images of carbon felt in the cathode (Fig. S5) revealed no dense biofilm formation for all three groups. These observations suggest that VFA production may primarily occur through the activity of suspended biomass in H_2-mediated electrosynthesis. Limitations in CO_2 conversion caused by low H_2 gas solubility and inefficient gas delivery to microorganisms could result in reduced FE for VFA production. Moreover, oxygen generated at the anode may diffuse from the anode chamber to the cathode, which is unavoidable even with an ion-exchange membrane separator. This diffusion could inhibit microbial activity and further decrease FE in MES [38]. To enhance the FE for VFA production, several strategies can be employed, including the promotion of H_2 transfer within the cathode chamber by incorporating gas transfer mediators, increasing microbial biomass in the cathode using slurry electrodes, and encouraging dense biofilm formation on the cathode surface [39,40].

3.3. Long-term operation of MES with nickel foam electrodes

The MES reactors with CF-NF cathodes showed the most promise, so they were operated for an extended 60 days at an applied cathode potential of −0.89 V for long-term testing. Catholyte was replaced by fresh medium on day 32 to start a new batch, but no methanogenic inhibitor was added during the test. Fig. 3a shows the MES production profile in the cathode chamber. Acetate remained to be the dominant product, and its concentration increased during each batch much more significantly than other product species. The maximum acetate production rates of 1.61 and 1.13 g L^{-1} d^{-1} were observed for batches 1 and 2, respectively, and the average production rate of 0.47 g L^{-1} d^{-1} (7.81 mM d^{-1}) was calculated during the two operation periods. The highest accumulating acetate concentration of 16.0 g L^{-1} was obtained at day 30 by the end of the first batch. Acetate accounted for 87.8% of all VFAs, which shows a good potential of such MES systems for selective acetate production with high titers. Other VFAs, including butyrate and formate, were also detected, but in a much lower concentration, and they also accumulated along with the operation. The concentration of butyrate in the final catholyte increased from 1.33 g L^{-1} for batch 1 to 2.87 g L^{-1} for batch 2, possibly due to some chain elongation level during long-term operation [15,41,42]. Similar to the short-term operation discussed above, we also found significant VFA diffusion from the cathode to the anode chamber (5.8 and 7.5 g L^{-1} acetate in batches 1 and 2, respectively).

Table S2 compares the performance of this study with the reported performance for acetate production in MES with cathodes

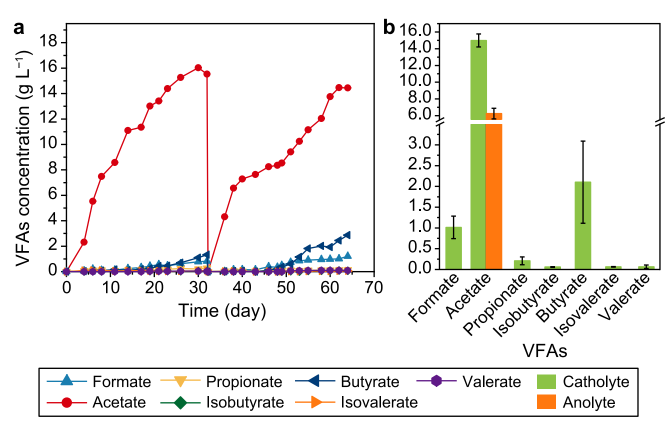

Fig. 3. VFA production in the long-term operation of MES with NF-CF cathode (**a**) and VFA distribution in the final electrolyte (**b**).

modified with nickel-based catalysts. Compared to many of the studies that used synthetic catalysts, this study showed much higher current density (19.25 ± 1.05 A m^{-2} during long-term operation test), averaged volumetric production rate of acetate (0.47 g L^{-1} d^{-1}), as well as resulted in maximum acetate titer of 16.0 g L^{-1}. The high titer in VFA production observed in this study compared to previous Ni-based cathodes may be attributed to several factors. A main contributor could be the higher current density delivered in this study resulting from the high conductivity of nickel foam compared with other nickel-coated carbon materials and the lower cathode potential applied in the study. In addition, the H_2-mediated process enables much faster microbial reaction kinetics in CO_2 reduction than surface-limited attached growth. Other influencing factors may include reactor configuration, microbial inoculum, and operation conditions. These results demonstrated that a higher VFA production rate and titer could be achieved using commercial nickel foam coupled carbon felt cathode without complex fabrications of new materials. The approaches presented in this study have potential applications in other electrosynthesis processes, facilitating the production of diverse VFAs or alcohols through indirect electron transfer via hydrogen [43,44]. Considering the diverse compounds generated in the cathode, additional purification strategies such as pervaporation, membrane distillation, and membrane contractors could be utilized based on the desired product and economic considerations [37,45,46]. However, Faradaic efficiency on VFA production is still low (~14.7%), which might be attributed to the partial utilization of H_2 by microbes for VFA production. Faradaic efficiency for electrosynthesis could be further improved by accelerating H_2 delivery to microbes, promoting suspended biomass growth to enhance CO_2 conversion [39,47]. In addition, methane production will also reduce Faradaic efficiency due to the consumption of acetate, H_2, or other electron donors, so methanogenesis inhibition is needed in such mixed culture systems.

3.4. Microscopic characterization and microbial community analysis

After long-term MES operation, microbes attached to the carbon felt and nickel foam electrode surface were analyzed using SEM (Fig. 4). There was no dense biofilm observed on the cathodes, suggesting that biofilm was not a prerequisite for VFA production in these MES systems despite high current density. This observation differed from previous studies using carbon felt, which showed biofilm with high density on electrodes [48,49]. Many factors affect cathode biofilm formation and growth, including microbial species, cathode potential, and pH [42,50]. The scarcity of biofilm on the cathode does support the hypothesis that extracellular electron transfer via direct contact did not play a major role in high titer VFA production in this study. Instead, the H_2-mediated pathway was responsible for such conversion. Hydrogen production on the surface of electrodes also inhibits biofilm growth due to shearing, which may also result in low biofilm coverage. The nickel foam of the hybrid cathode exhibited a stable mechanical structure after long-term operation compared to the control material (Fig. S7). However, it is worth noting that catholyte pH should be maintained around neutral to allow microbial activities and prevent nickel leaking [51]. Such leaking may harm microbes in the cathode by binding to proteins or enzymes, damaging the phospholipid membrane or genetic materials, consequently reducing VFA production [52].

To investigate the microbial community structures, microbial samples of inoculum, cathode-attached cells, and bulk catholyte were analyzed using high-throughput 16S rRNA gene sequencing. The dominant microbial community shifted from the initial inoculum to the end of the MES operation (Fig. 5). At the genus level, *Acetobacterium* was dominant, and its abundance increased from 32.1% in the inoculum to 73.2% on the MES cathode after 14 days. In contrast, no obvious change was found in the suspension of catholyte (29.9%). *Acetobacterium* is a genus of autotrophic acetogens that produce acetate through the Wood-Ljungdahl pathway. As a high rate of H_2 was produced directly on the cathode, the acetogenesis community could be easily enriched on the electrode. In addition to acetate, *Acetobacterium* has been reported to express a fatty acid chain-elongation pathway and produce butyrate, which may explain the small amounts of butyrate accumulation in this study [53].

After a long-term operation of over 60 days, *Acetobacterium* remained a dominant genus, but the abundance slowly reduced to 20.9% on the cathode-attached cells. In contrast, a gradual increase in *Methanobrevibacter* was also identified. *Methanobrevibacter* is a hydrogenotrophic archaea that converts CO_2 and H_2 into CH_4. Since the study focuses on mixed culture reactions, it is understandable that methanogenesis would develop after a period, though not initially. *Methanobrevibacter* has high H_2 affinity, so once established, it could convert CO_2 and H_2 to CH_4 and reduce the overall Faradaic efficiency. In MES, the evolution of H_2 can lead to an

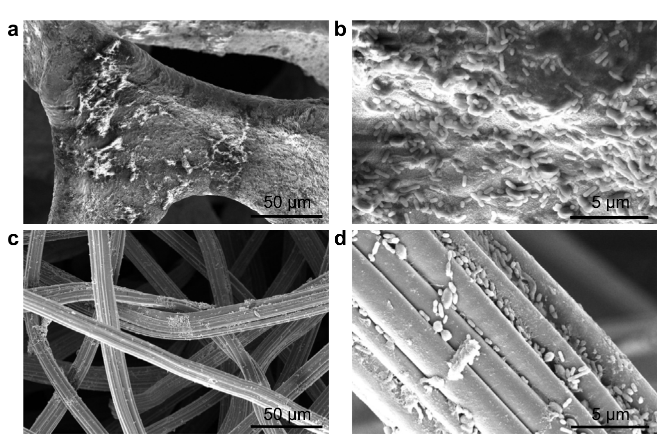

Fig. 4. Microscopic characterizations of nickel foam (**a**, 50 μm scale; **b**, 5 μm scale) and carbon felt (**c**, 50 μm scale; **d**, 5 μm scale) after long-term operation.

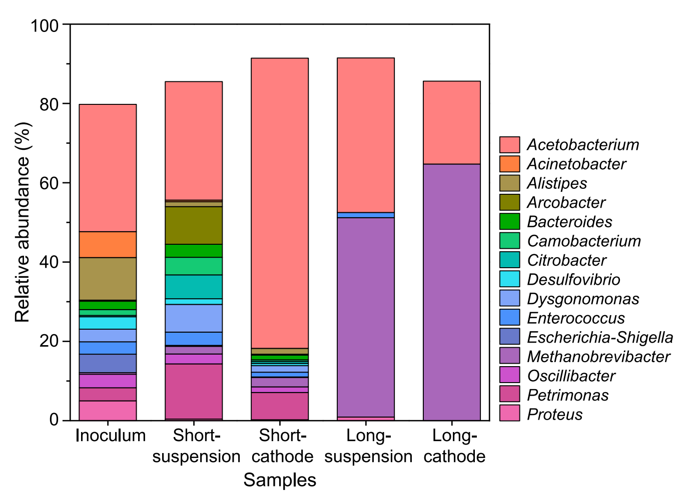

Fig. 5. Composition of the microbial community on the cathode and catholyte compared with initial inoculum in genus level. Short-refers to samples collected from MES operated with a 14-day cycle, and Long-refers to samples collected after 64-day operation.

increase in pH due to the consumption of protons, while the formation of VFAs can cause a decrease in pH within the catholyte. During the long-term operation tests, the catholyte pH experienced a slight increase from ~7.0 to ~7.5 (Fig. S6). The increase can be attributed to the continuous consumption of protons for H_2 production and the buffering effect of H_2CO_3, which occurs because of ongoing CO_2 gas purging in the catholyte. The pH values reported in the literature are influenced by various factors, such as the specific microbes, reactor configuration, inorganic carbon sources, and the products being generated [33,43,54]. The presence of *Methanobrevibacter* could also explain the low FE observed for VFA production. At the end of the long-term experiment, the methane gas content was 0.7–2.1% of the off gas. Regrettably, we didn't perform a quantitative evaluation of FE on methane production, as methane products only occurred after long-term operation, and we didn't measure methane regularly. This was partially because methanogenesis inhibitor sodium 2-bromoethanesulfonate (BES, 1 g L^{-1}) was added during the operation and proved effective for most of the operation duration. A previous study demonstrated complete inhibition of methanogenesis by applying a high concentration of 50 mM of 2-Bromoethanesulfonate (10 g L^{-1}) [55]. However, it may not be considered sustainable, primarily due to the high cost and potential toxicity to the beneficial microbes. Many methods could be applied for methanogenesis inhibition in microbial electrochemical systems, such as pH control, the use of heat-pretreated inoculum, temperature control, and so forth [56,57].

4. Conclusions

Indirect electron transfer through H_2 is hypothesized to hold a much higher near-term potential for high-titer volatile fatty acids production from microbial electrosynthesis systems. This investigation substantiates this potential by employing commercial nickel foam coupled with carbon felt cathodes in mixed culture MES reactors. A high acetate concentration (14.4–16.0 g L^{-1}) was obtained in lab-scale fed-batch reactors, among the highest reported in the literature. Meanwhile, acetate back diffusion from the cathode to the anode chamber was detected due to the concentration gradient between chambers. With excess *in situ* H_2 supply on the cathode, acetate was produced at a high rate of 2.0 g L^{-1} d^{-1}. *Acetobacterium* was found to be dominant in the microbes attached to the cathode (73.2% relative abundance) and catholyte suspension (29.9% relative abundance). Simultaneously, there is a gradual enrichment of the hydrogenotrophic methanogen *Methanobrevibacter*. To advance this field, further studies should focus on minimizing cross-chamber losses of liquid products and mitigating methanogenesis while maintaining high selectivity and titer production of acetate.

CRediT authorship contribution statement

Yanhong Bian: Conceptualization, Methodology, Investigation, Formal Analysis, Validation, Visualization, Writing - Original Draft, Writing - Review & Editing. **Aaron Leininger:** Methodology, Formal Analysis. **Harold D. May:** Writing - Review & Editing. **Zhiyong Jason Ren:** Conceptualization, Funding Acquisition, Project Administration, Supervision, Validation, Writing - Review & Editing.

Declaration of competing interest

The authors declare that they have no known competing financial interests or personal relationships that could have appeared to influence the work reported in this paper.

Acknowledgements

This work is supported by the Department of Energy Bioenergy Technologies Office under the award DE-EE0008932. The authors acknowledge the use of Princeton's Imaging and Analysis Center, which is partially supported through the Princeton Center for Complex Materials (PCCM), a National Science Foundation (NSF)-MRSEC program (DMR-2011750). The authors thank the Lewis-Sigler Institute for Integrative Genomics for assistance with library preparation and high-throughput sequencing.

Appendix A. Supplementary data

Supplementary data to this article can be found online at https://doi.org/10.1016/j.ese.2023.100324.

References

[1] S. Bouckaert, A.F. Pales, C. McGlade, U. Remme, B. Wanner, L. Varro, D. D'Ambrosio, T. Spencer, Net Zero by 2050: A Roadmap for the Global Energy Sector, 2021.
[2] L. Lu, J.S. Guest, C.A. Peters, X. Zhu, G.H. Rau, Z.J. Ren, Wastewater treatment for carbon capture and utilization, Nat. Sustain. 1 (12) (2018) 750–758.
[3] A. Kätelhön, R. Meys, S. Deutz, S. Suh, A. Bardow, Climate change mitigation potential of carbon capture and utilization in the chemical industry, Proc. Natl. Acad. Sci. USA 116 (23) (2019) 11187–11194.
[4] Y. Jiang, H.D. May, L. Lu, P. Liang, X. Huang, Z.J. Ren, Carbon dioxide and organic waste valorization by microbial electrosynthesis and electrofermentation, Water Res. 149 (2019) 42–55.
[5] K.P. Nevin, T.L. Woodard, A.E. Franks, Z.M. Summers, D.R. Lovley, Microbial electrosynthesis: feeding microbes electricity to convert carbon dioxide and water to multicarbon extracellular organic compounds, mBio 1 (2) (2010) e00103-00110.
[6] E. Blanchet, F. Duquenne, Y. Rafrafi, L. Etcheverry, B. Erable, A. Bergel, Importance of the hydrogen route in up-scaling electrosynthesis for microbial CO2reduction, Energy Environ. Sci. 8 (12) (2015) 3731–3744.
[7] X. Zhu, J. Jack, A. Leininger, M. Yang, Y. Bian, J. Lo, W. Xiong, N. Tsesmetzis, Z.J. Ren, Syngas mediated microbial electrosynthesis for CO2 to acetate conversion using Clostridium ljungdahlii, Resour. Conserv. Recycl. 184 (2022) 106395.
[8] E. Perona-Vico, L. Feliu-Paradeda, S. Puig, L. Bañeras, Bacteria coated cathodes as an in-situ hydrogen evolving platform for microbial electrosynthesis, Sci Rep-Uk 10 (1) (2020) 19852.
[9] D.R. Lovley, K.P. Nevin, Electrobiocommodities: powering microbial production of fuels and commodity chemicals from carbon dioxide with electricity, Curr. Opin. Biotechnol. 24 (3) (2013) 385–390.
[10] G. Mohanakrishna, J.S. Seelam, K. Vanbroekhoven, D. Pant, An enriched electroactive homoacetogenic biocathode for the microbial electrosynthesis of acetate through carbon dioxide reduction, Faraday Discuss 183 (2015) 445–462, 0.
[11] S. Das, S. Das, M.M. Ghangrekar, Application of TiO2 and Rh as cathode catalyst to boost the microbial electrosynthesis of organic compounds through CO2 sequestration, Process Biochem. 101 (2021) 237–246.
[12] S. Tian, H. Wang, Z. Dong, Y. Yang, H. Yuan, Q. Huang, T.-s. Song, J. Xie, Mo2C-induced hydrogen production enhances microbial electrosynthesis of acetate from CO2 reduction, Biotechnol. Biofuels 12 (1) (2019) 71.
[13] A. Prévoteau, J.M. Carvajal-Arroyo, R. Ganigué, K. Rabaey, Microbial electrosynthesis from CO2: forever a promise? Curr. Opin. Biotechnol. 62 (2020) 48–57.
[14] S. Gildemyn, K. Verbeeck, R. Slabbinck, S.J. Andersen, A. Prévoteau, K. Rabaey, Integrated production, extraction, and concentration of acetic acid from CO2 through microbial electrosynthesis, Environ. Sci. Technol. Lett. 2 (11) (2015) 325–328.
[15] L. Jourdin, M. Winkelhorst, B. Rawls, C.J. Buisman, D.P. Strik, Enhanced selectivity to butyrate and caproate above acetate in continuous bioelectrochemical chain elongation from CO2: steering with CO2 loading rate and hydraulic retention time, Bioresour. Technol. Rep. 7 (2019) 100284.
[16] X. Ma, G.Q. Zhang, F.T. Li, M.Y. Jiao, S.Y. Yao, Z.P. Chen, Z.Y. Liu, Y.Y. Zhang, M. Lv, L.C. Liu, Boosting the microbial electrosynthesis of acetate from CO2 by hydrogen evolution catalysts of Pt nanoparticles/rGO, Catal. Lett. (2021) 11.
[17] J. Tang, Y. Bian, S. Jin, D. Sun, Z.J. Ren, Cathode material development in the past decade for H2 production from microbial electrolysis cells, ACS Environ. Au 2 (1) (2021) 20–29.
[18] M. Tabish Noori, B. Min, Highly porous FexMnOy microsphere as an efficient cathode catalyst for microbial electrosynthesis of volatile fatty acids from CO2, Chemelectrochem 6 (24) (2019) 5973–5983.
[19] F. Kracke, A.B. Wong, K. Maegaard, J.S. Deutzmann, M.A. Hubert, C. Hahn, T.F. Jaramillo, A.M. Spormann, Robust and biocompatible catalysts for efficient hydrogen-driven microbial electrosynthesis, Commun. Chem. 2 (1) (2019) 45.

[20] T.s. Song, K. Fei, H. Zhang, H. Yuan, Y. Yang, P. Ouyang, J. Xie, High efficiency microbial electrosynthesis of acetate from carbon dioxide using a novel graphene−nickel foam as cathode, J. Appl. Chem. Biotechnol. 93 (2) (2018) 457−466.
[21] B. Bian, J. Xu, K.P. Katuri, P.E. Saikaly, Resistance assessment of microbial electrosynthesis for biochemical production to changes in delivery methods and CO2 flow rates, Bioresour. Technol. 319 (2021) 124177.
[22] M.d.P.A. Rojas, M. Zaiat, E.R. González, H. De Wever, D. Pant, Enhancing the gas−liquid mass transfer during microbial electrosynthesis by the variation of CO2 flow rate, Process Biochem. 101 (2021) 50−58.
[23] Y. Matsumoto, E. Sato, Electrocatalytic properties of transition metal oxides for oxygen evolution reaction, Mater. Chem. Phys. 14 (5) (1986) 30.
[24] T. Audichon, T.W. Napporn, C. Canaff, C. Morais, C. Comminges, K.B. Kokoh, IrO2 coated on RuO2 as efficient and stable electroactive nanocatalysts for electrochemical water splitting, J. Phys. Chem. C 120 (5) (2016) 2562−2573.
[25] D. Bagchi, S. Sarkar, A.K. Singh, C.P. Vinod, S.C. Peter, Potential- and time-dependent dynamic nature of an oxide-derived PdIn nanocatalyst during electrochemical CO2 reduction, ACS Nano 16 (4) (2022) 6185−6196.
[26] J. Jiang, X. Chen, X. Chen, Z.J. Ren, Energy-efficient microbial electrochemical lignin and alkaline hydroxide recovery from DMR black liquor, Resour. Conserv. Recycl. 186 (2022) 106529.
[27] S.E. Fratesi, F.L. Lynch, B.L. Kirkland, L.R. Brown, Effects of SEM preparation techniques on the appearance of bacteria and biofilms in the Carter Sandstone, J. Sediment. Res. 74 (6) (2004) 858−867.
[28] A. Leininger, Z.J. Ren, Circular utilization of food waste to biochar enhances thermophilic co-digestion performance, Bioresour. Technol. 332 (2021) 125130.
[29] B.J. Callahan, P.J. McMurdie, M.J. Rosen, A.W. Han, A.J.A. Johnson, S.P. Holmes, DADA2: high-resolution sample inference from Illumina amplicon data, Nat. Methods 13 (7) (2016) 581−583.
[30] C. Quast, E. Pruesse, P. Yilmaz, J. Gerken, T. Schweer, P. Yarza, J. Peplies, F.O. Glöckner, The SILVA ribosomal RNA gene database project: improved data processing and web-based tools, Nucleic Acids Res. 41 (D1) (2012) D590−D596.
[31] P.J. McMurdie, S. Holmes, phyloseq: an R package for reproducible interactive analysis and graphics of microbiome census data, PLoS One 8 (4) (2013) e61217.
[32] S. Shiva Kumar, H. Lim, An overview of water electrolysis technologies for green hydrogen production, Energy Rep. 8 (2022) 13793−13813.
[33] G. Mohanakrishna, K. Vanbroekhoven, D. Pant, Imperative role of applied potential and inorganic carbon source on acetate production through microbial electrosynthesis, J. CO2 Util. 15 (2016) 57−64.
[34] S. Bajracharya, A. ter Heijne, X.D. Benetton, K. Vanbroekhoven, C.J.N. Buisman, D.P.B.T.B. Strik, D. Pant, Carbon dioxide reduction by mixed and pure cultures in microbial electrosynthesis using an assembly of graphite felt and stainless steel as a cathode, Bioresour. Technol. 195 (2015) 14−24.
[35] B. Bian, M.F. Alqahtani, K.P. Katuri, D. Liu, S. Bajracharya, Z. Lai, K. Rabaey, P.E. Saikaly, Porous nickel hollow fiber cathodes coated with CNTs for efficient microbial electrosynthesis of acetate from CO2 using Sporomusa ovata, J. Mater. Chem. A 6 (35) (2018) 17201−17211.
[36] S. Gildemyn, K. Verbeeck, R. Jansen, K. Rabaey, The type of ion selective membrane determines stability and production levels of microbial electrosynthesis, Bioresour. Technol. 224 (2017) 358−364.
[37] X. Zhu, A. Leininger, D. Jassby, N. Tsesmetzis, Z.J. Ren, Will membranes break barriers on volatile fatty acid recovery from anaerobic digestion? ACS ES&T Eng. 1 (1) (2020) 141−153.
[38] M. Abdollahi, S. Al Sbei, M.A. Rosenbaum, F. Harnisch, The oxygen dilemma: the challenge of the anode reaction for microbial electrosynthesis from CO2, Front. Microbiol. (2022) 2819.
[39] X. Xue, Z. Liu, W. Cai, K. Cui, K. Guo, Porous polyurethane particles enhanced the acetate production of a hydrogen-mediated microbial electrosynthesis reactor, Bioresour. Technol. Rep. 18 (2022) 101073.
[40] Y. Jiang, Q. Liang, N. Chu, W. Hao, L. Zhang, G. Zhan, D. Li, R.J. Zeng, A slurry electrode integrated with membrane electrolysis for high-performance acetate production in microbial electrosynthesis, Sci. Total Environ. 741 (2020) 140198.
[41] I. Vassilev, P.A. Hernandez, P. Batlle-Vilanova, S. Freguia, J.O. Krömer, J.r. Keller, P. Ledezma, B. Virdis, Microbial electrosynthesis of isobutyric, butyric, caproic acids, and corresponding alcohols from carbon dioxide, ACS Sustain. Chem. Eng. 6 (7) (2018) 8485−8493.
[42] P. Izadi, J.-M. Fontmorin, A. Godain, E.H. Yu, I.M. Head, Parameters influencing the development of highly conductive and efficient biofilm during microbial electrosynthesis: the importance of applied potential and inorganic carbon source, Npj Biofilms Microbi 6 (1) (2020) 1−15.
[43] R. Ganigue, S. Puig, P. Batlle-Vilanova, M.D. Balaguer, J. Colprim, Microbial electrosynthesis of butyrate from carbon dioxide, Chem. Commun. 51 (15) (2015) 3235−3238.
[44] P. Izadi, J.-M. Fontmorin, B. Virdis, I.M. Head, E.H. Yu, The effect of the polarised cathode, formate and ethanol on chain elongation of acetate in microbial electrosynthesis, Appl. Energy 283 (2021) 116310.
[45] M. Yang, J.-J. Zhu, A. McGaughey, S. Zheng, R.D. Priestley, Z.J. Ren, Predicting extraction selectivity of acetic acid in pervaporation by machine learning models with data leakage management, Environ. Sci. Technol. 57 (14) (2023) 5934−5946.
[46] P. Batlle-Vilanova, R. Ganigue, S. Ramio-Pujol, L. Baneras, G. Jimenez, M. Hidalgo, M.D. Balaguer, J. Colprim, S. Puig, Microbial electrosynthesis of butyrate from carbon dioxide: production and extraction, Bioelectrochemistry 117 (2017) 57−64.
[47] R.M. Rodrigues, X. Guan, J.A. Iñiguez, D.A. Estabrook, J.O. Chapman, S. Huang, E.M. Sletten, C. Liu, Perfluorocarbon nanoemulsion promotes the delivery of reducing equivalents for electricity-driven microbial CO2 reduction, Nat. Catal. 2 (5) (2019) 407−414.
[48] F. Ameen, W.A. Alshehri, S.A. Nadhari, Effect of electroactive biofilm formation on acetic acid production in anaerobic sludge driven microbial electrosynthesis, ACS Sustain. Chem. Eng. 8 (1) (2019) 311−318.
[49] N. Aryal, A. Halder, P.-L. Tremblay, Q. Chi, T. Zhang, Enhanced microbial electrosynthesis with three-dimensional graphene functionalized cathodes fabricated via solvothermal synthesis, Electrochim. Acta 217 (2016) 117−122.
[50] Q. Li, Q. Fu, H. Kobayashi, Y. He, Z. Li, J. Li, Q. Liao, X. Zhu, GO/PEDOT modified biocathodes promoting CO 2 reduction to CH 4 in microbial electrosynthesis, Sustain. Energy Fuels 4 (6) (2020) 2987−2997.
[51] S. Das, P. Chatterjee, M. Ghangrekar, Increasing methane content in biogas and simultaneous value added product recovery using microbial electrosynthesis, Water Sci. Technol. 77 (5) (2018) 1293−1302.
[52] Y. Gao, Z. Li, J. Cai, L. Zhang, Q. Liang, Y. Jiang, R.J. Zeng, Metal nanoparticles increased the lag period and shaped the microbial community in slurry-electrode microbial electrosynthesis, Sci. Total Environ. 838 (2022) 156008.
[53] E.V. LaBelle, C.W. Marshall, H.D. May, Microbiome for the electrosynthesis of chemicals from carbon dioxide, Acc. Chem. Res. 53 (1) (2020) 62−71.
[54] G. Mohanakrishna, I.M.A. Reesh, K. Vanbroekhoven, D. Pant, Microbial electrosynthesis feasibility evaluation at high bicarbonate concentrations with enriched homoacetogenic biocathode, Sci. Total Environ. 715 (2020) 137003.
[55] S. Zinder, T. Anguish, S. Cardwell, Selective inhibition by 2-bromoethanesulfonate of methanogenesis from acetate in a thermophilic anaerobic digestor, Appl. Environ. Microbiol. 47 (6) (1984) 1343−1345.
[56] K. He, W. Li, L. Tang, W. Li, S. Lv, D. Xing, Suppressing methane production to boost high-purity hydrogen production in microbial electrolysis cells, Environ. Sci. Technol. 56 (17) (2022) 11931−11951.
[57] D.A. Jadhav, A.D. Chendake, A. Schievano, D. Pant, Suppressing methanogens and enriching electrogens in bioelectrochemical systems, Bioresour. Technol. 277 (2019) 148−156.